Fundamental Environmental Reactivity Testing and Analysis of the Hydrogen Storage Material $2LiBH_4 \cdot MgH_2$

Charles W. James Jr, Kyle S. Brinkman, Joshua R. Gray,
Jose A. Cortes-Concepcion & Donald L. Anton*

Savannah River National Laboratory
Aiken, SC, 29808 USA,

* Corresponding Author: Tel: +1 803-507-8551, Fax: +1 803-652-8137
Email: *donald.anton@srnl.doe.gov*

Abstract

While the storage of hydrogen for portable and stationary applications is regarded as critical in bringing PEM fuel cells to commercial acceptance, little is known of the environmental exposure risks posed in utilizing condensed phase chemical storage options as in complex hydrides. It is thus important to understand the effect of environmental exposure of metal hydrides in the case of accident scenarios. Simulated tests were performed following the United Nations standards to test for flammability and water reactivity in air for a destabilized lithium borohydride and magnesium hydride system in a 2 to 1 molar ratio respectively. It was determined that the mixture acted similarly to the parent, lithium borohydride, but at slower rate of reaction seen in magnesium hydride. To quantify environmental exposure kinetics, isothermal calorimetry was utilized to measure the enthalpy of reaction as a function of exposure time to dry and humid air, and liquid water. The reaction with liquid water was found to increase the heat flow significantly during exposure compared to exposure in dry or humid air environments. Calorimetric results showed the maximum normalized heat flow the fully charged material was 6 mW/mg under liquid phase hydrolysis; and 14 mW/mg for the fully discharged material also occurring under liquid phase hydrolysis conditions.

Keywords: hydrogen storage, environmental reactivity, lithium borohydride, magnesium hydride, calorimetry

1. Introduction

The storage of hydrogen in a volumetrically and gravimetrically dense form must be met for the realization of hydrogen powered light duty vehicles. There have been numerous studies focused on understanding the sorption kinetics, hydrogen capacity and structures of the three primary types of complex metal hydrides: alanates[1-3], borohydrides [4-6], and amides [7-9]. However, there is very little understanding of the potential environmental exposure risks associated with implementing these materials. Therefore, it is important to understand and quantify these risks in the case of a storage tank being breached and the hydride material exposed to conditions such as dry air, humid air, liquid water and simultaneous water/air contact.

There are a number of recent publications that have begun to explore the risks of environmental exposure of catalyzed $NaAlH_4$ and similar mateirals materials [11-13] which have been used in kilogram quantities in laboratory demonstrations of stoprage systems. In these studies, liquid or gaseous water contact has been identified as leading to the most vigerous reactions resutling in hydrogen gas releas and heat generation. The controlled hydrolysis of chemical hydrides such as sodium borohydride have been studied for hydrogen generation, however much less is understood about uncontrolled hydrolysis and oxidation under accidental environmental exposure scenarios. For example, the oxidation behavior of alkali hydride LiH has been investigated [19] focusing on trace amounts of O_2 and H_2O reactants which can oxidize the LiH surface and inhibit the material from its role in successfully reacting with ammonia gas generated from lithium amide decomposition. Concerning studies focused on the safety of materials and properties for engineering storage systems, a report written by Dedrick [20] compiled data on the sodium alanate, $NaAlH_4$, system including the identification of gas and solid products resulting from air and water exposure.

This paper will focus on another chemical hydride system which has been shown to be reversible; a mixture of lithium borohydride ($LiBH_4$) and magnesium hydride (MgH_2) in a molar ratio of 2 to 1, respectively. Vajo et al[14] showed that the formation of MgB_2 during dehydrogenation reduced the enthalpy of reaction making the material reversiable at 1-10 bar and 20-100°C. The "destabilized" mixture has been reported to have a >10wt% H_2 capacity. [14, 15]. The reversible chemical reaction was given as:

$$LiBH_4 + \tfrac{1}{2} MgH_2 \leftrightarrow LiH + \tfrac{1}{2} MgB_2 + 2H_2 \qquad (1).$$

This paper will outline the results of a series of tests following the United Nation procedures for testing of water reactivity and flammability testing. In addition to these qualitative experiments, a quantitative assessment of the rate of heat released during air and water exposure were undertaken utilizing a Calvet calorimeter.

2. Experimental Details

2.1 Material Preparation

The starting materials, lithium borohydride ($\geq$ 90%, Sigma Aldrich) and magnesium hydride (>95%, Alfa Aesar) were purchased and used as-received. Approximately three grams of the 2:1 molar mixture of $LiBH_4$:MgH_2 were loaded into a milling jar within an argon filled glove box. The samples were prepared using a Spex mill for 1 hour. A ball-to-sample ratio of 20 gm to 3 gm was maintained for all samples.

2.2 U.N. Testing

A set of materials testing procedures was developed based on internationally accepted United Nations testing procedures [21]. These tests include exposure to laboratory air, and liquid water and fully described in the following sections. These U.N. test procedures were modified by inclusion of thermocouples to monitor the temperature in proximity to or within

the test material, All tests were video recorded for later analysis and comparison.

2.2.1 Water Reactivity

The purpose of the water reactivity test is to identify if the substance, when in contact with water, burns or emits flammable gases. If spontaneous ignition occurred at any stage, the substance is classified as a water reactive substance emitting flammable gases. The experimental details followed UN-RTDG part-3, test-N5 in which three separate tests were conducted. (i) The test substance was formed into a small uniform pile approximately 20 mm high and 30 mm diameter with a hollow in the top to catch water. A few drops of water are added to the hollow with a pipette. (*Water Drop Test*) (ii) A small quantity (approximately 2 mm diameter) of the test substance was dropped in a beaker of distilled water at 20^{o}C. (*Water Immersion Test)* (iii) A small quantity (approximately 2 mm diameter) of the test substance was placed on the center of a filter paper which is floated flat on the surface of distilled water at 20^{o}C in a 250 ml beaker. The filter paper keept the substance simultaneously in contact with water and air, under which the likelihood of spontaneous ignition of any evolved gas is greatest. (*Surface Contact Test*)

2.2.2 Flammability Test

Burn Rate Test

The purpose of the burn rate test is to classify rapidly combustible solids by differentiation between ignitable, rapid burning and dangerous burning substances and to assess the relative hazards of rapidly combustible solids. The test procedure details followed UN-RTDG part-3, test-N1. The sample material was deposited as a strip on a platform to measure the burning rate. The strip 250 mm in length and 100 mm^2 cross-section was ignited from one end and the burn propagation time measured for 100 mm after an initial stabilization period. A series of 6 thermocouples were fitted along the powder strip length at regular intervals, so that the

temperature approximately could be monitored as a function of time. Additionally, these tests were video recorded to provide qualitative data acquisition, as well as to calculate the burn rate.

Spontaneous Combustion Test

This test is conducted in order to determine the susceptibility of a material to spontaneously ignite in air if subjected to an elevated temperature. The details of the test procedure followed UN-RTDG div. 4.2. The powder samples were loaded in 25x25x25mm stainless steel mesh baskets with 0.05 mm mesh openings and an uncovered top surface. Three chromel-alumel thermocouples, with 0.3 mm diameter were inserted into the cubic sample container at positions in the cube center, face-center, and cube corner to monitor temperature. The basket was housed in a secondary enclosed cubic mesh container also made of stainless steel with a mesh opening of 0.60 mm, and slightly larger than the sample container. The cube was set in a hot air circulating oven nominally at 150^{o}C for at least 24 hours or until spontaneous ignition or hazardous self-heating was observed. It was experimentally observed that there was a measured 10^{o}C overshoot above the nominal set-point temperature. The changes of sample temperature at the chosen locations of the cube were recorded for the duration of the test.

Pyrophoricity Test

The purpose of the pyrophoricity test is to determine the ability of a powder solid to ignite on contact with air and determine the time to ignition. The test procedure followed UN-RTDG part-3, test-N2. A 1~2 ml sample was poured from approximately a one meter height onto a non-combustible surface. Observation was made as to whether the substance ignited during dropping or within 5 minutes of settling. This procedure was performed six times or until a positive result was obtained. The substance was classified as *pyrophoric* if ignition occurred during one of three free-dropping tests.

2.3 Calorimetry

To quantify the heat released through contact with dry and humidified air and liquid water, oxidation and hydrolysis studies were performed in a Calvet calorimeter as described in [22, 23] The heat flow (mW) was normalized with respect to a nonexposed hydride and recorded versus time. Liquid water exposure tests were performed using a mixing cell with 1 ml of pH-neutral water to react with 5-10 mg of solid. Controlled humid air reaction measurements were conducted at varying relative humidity levels (30 and 60% RH) and temperatures (40 and 70 ^{o}C). For these measurements, the calorimeter equipped with a flow cell utlilizing either argon or air as the carrier gas with a flow rate of 10 ml/min reacting with 5-10 mg of solid.

There are important experimental differences for the exposure of hydrogen storage materials to water vapor versus liquid water in the calorimetric method used in this study. As graphically depicted in Figure 1a, at time = 0s in a liquid water mixing experiment, an excess of 32 times the stoichiometric amount of water was added which remained constant during the duration of the experiment. In contrast, the amount of water added during gas flow experiments was determined by the flow rate, the gas and reaction temperature and thermodynamics of the

water liquid/vapor equilibrium expressed through the relative humidity indicator. Since water vapor was added in a flow through configuration, the quantity provided for the hydrolysis reaction increased linearly with time. The saturation vapor pressure of water increases with temperature so that higher temperatures and higher relative humidity levels increased the amount of water available for the hydrolysis reaction. Figure 1b gives an expanded view of the time to stoichiometric water addition with varying temperature and relative humidity. The temperature of 40°C (104°F) represents conditions on a comfortable (60% relative humidity) and dry (30% relative humidity) summer day. The higher temperature, 70°C, was studied in order to estimate the effect of heat from a fuel cell or internal combustion engine operating at elevated temperatures in an accident scenario.

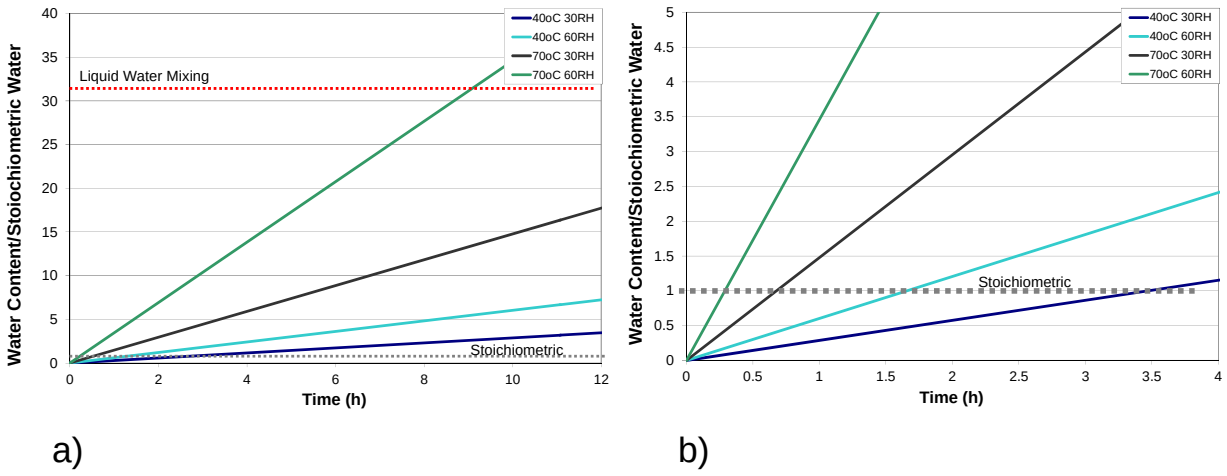

Figure 1 - Water content/Stoichiometric water versus time in hours (h) for gas phase hydrolysis in a flow cell with a flow rate of 10 ml/min at 40°C and 70°C with relative humidity levels of 30% and 60%. For liquid water mixing 32 times the stoichiometric water level is added at t=0.

3.0 Results and Discussion

3.1 U.N. Testing

The pure components, $LiBH_4$ and MgH_2, were first subjected to the series of U.N. Testing for water reactivity. It is of importance to understand that $LiBH_4$ is known to be hydrophilic, while MgH_2 is known to be hydrophobic. The phobicity affects the extent of reaction that can occur during environmental exposure. Figures 2 and 3, pictorially display the results of the Surface Contact and Water Drop test, respectively, for MgH_2 and $LiBH_4$. Keep in mind, the Surface Contact test utilizes the same volume of water used as in the Water Immersion test. The difference is a standard laboratory filter paper that is placed on top of the beaker of water, with direct contact beneath the liquid phase. This has the effect of ensuring that the hydride material is kept in a single location while in contact with the excess of water. Also, it reduces the heat transfer from the location of gas evolution into the water phase, as the material is now surrounded on the top and sides by less conductive air. It can be seen in Figure 2a that after a few seconds of exposure, MgH_2 undergoes a reaction event with the water and both the materials and any evolved hydrogen continue to burn for several minutes until the reactants are depleted. In comparison to this behavior, the $LiBH_4$ reacts immediately upon being placed on the filter paper, Figure 2b, and is observed to be much more reactive than MgH_2. The period of time over which the reaction continues is also much shorter, most likely due to the relatively strong reactivity.

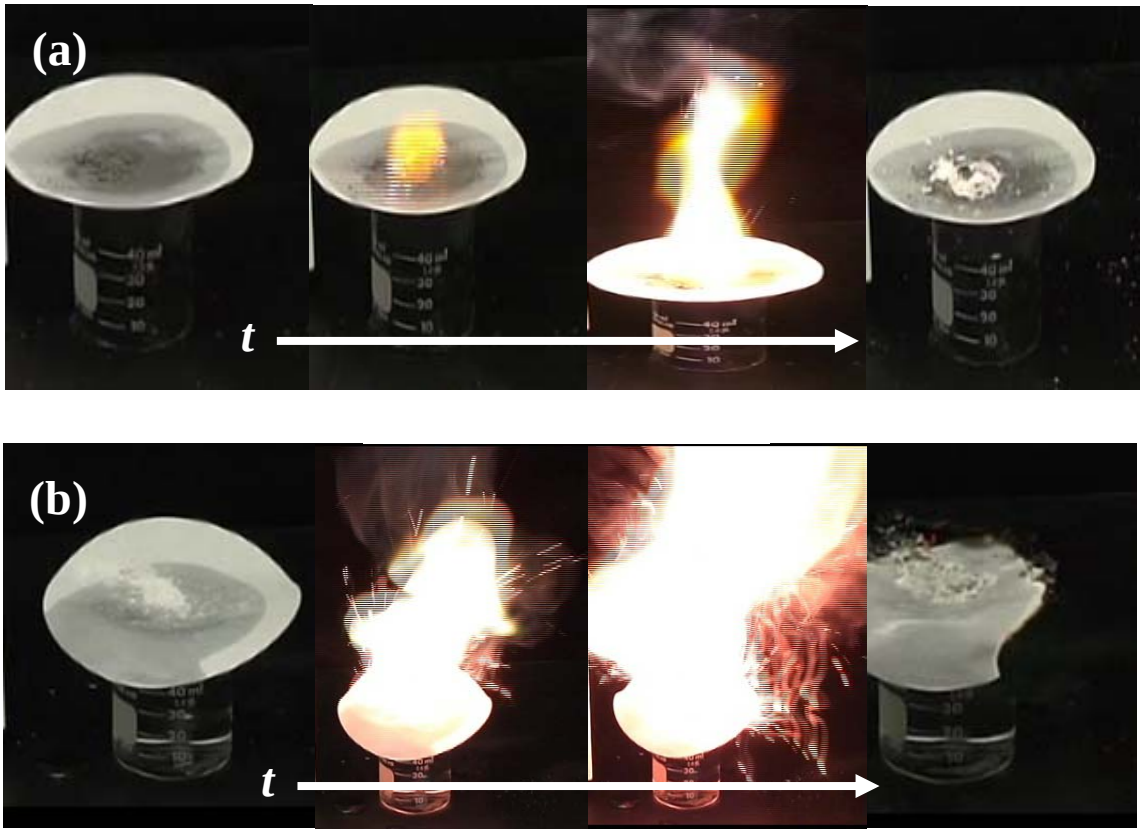

Figure 2 - Results of the Surface Contact Test for (a) MgH_2 and (b) $LiBH_4$ Showing Near-Instantaneous Reaction. Time Increases from Left to Right.

The final water reactivity test is the Water Drop test, wherein a few drops of water are added to a small conical pile of material. In this case, the hydride material is present in excess of the amount of water theoretically required to fully react via hydrolysis. It can be seen that MgH_2, Figure 3a required several drops of water to react, with the first several drops forming small balls of material that rolled off to the side due to the hydrophobic nature. After several attempts, a ball rested on top of the conical pile and this orientation led to the observed reactivity. This material continued to burn for several minutes, after which an ashen pile remained. In comparison, the $LiBH_4$, Figure 3b, material reacted nearly instantaneously in a much stronger event compared to the MgH_2. The observed sparks are most likely caused by the burning of the lithium itself.

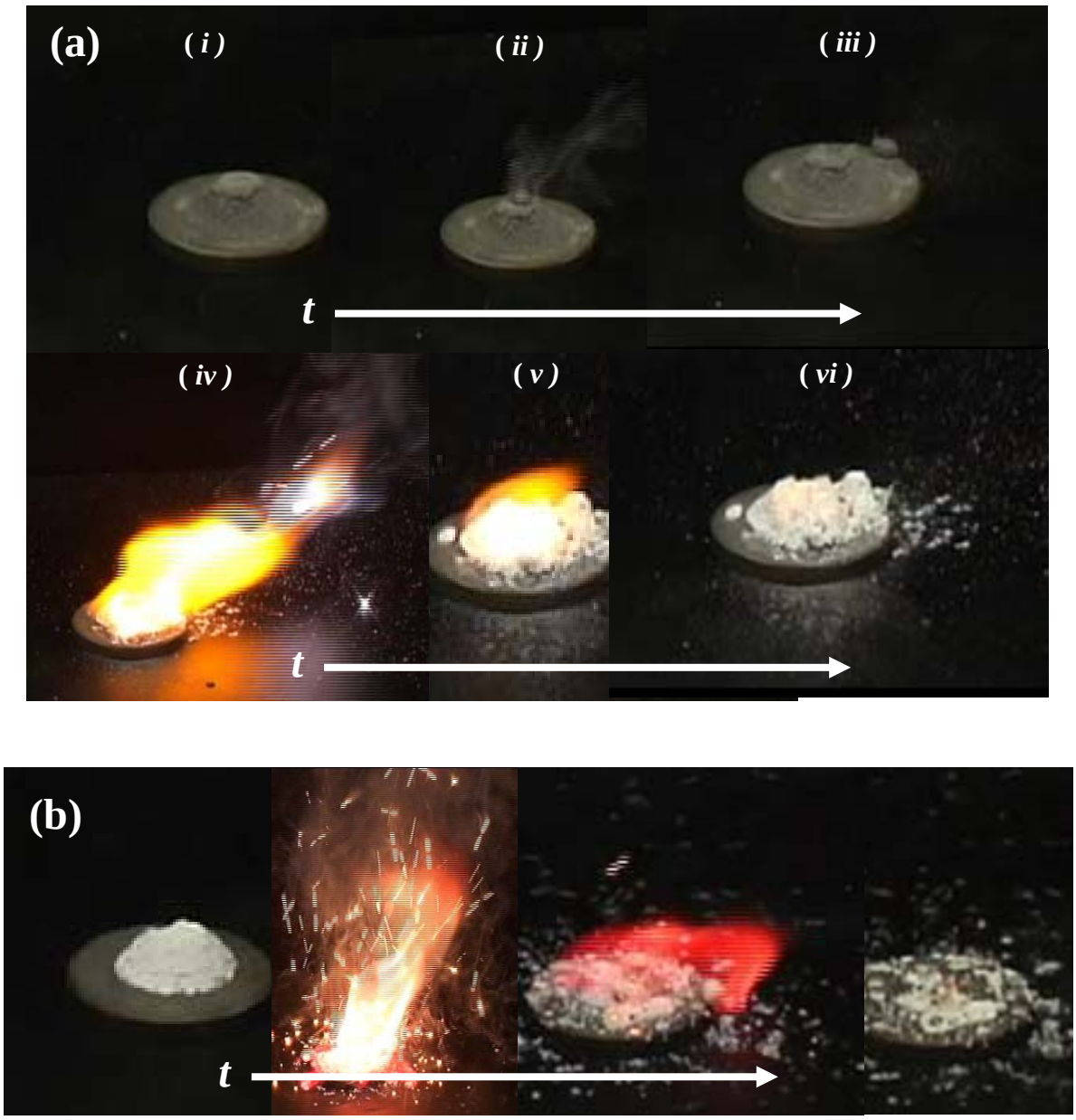

Figure 3 - Results of the Water Drop Test for (a) MgH_2 and (b) $LiBH_4$. Time Increases from Left to Right.

In the case of the fully charged, destabilized $2LiBH_4 \cdot MgH_2$ the same tests were performed. The results of water reactivity are shown in Figure 4. From Figure 4a, Water Immersion test, the material tends to form a film on the surface of the water, with very small spark-like events noted in some cases. At longer times, gas is evolved from the materials in the

film. This is consistent with the expectations of $2LiBH_4 \cdot MgH_2$ because the reactivity fell between the reactivity behavior of the parent MgH_2 and $LiBH_4$. The film-like formation is similar to that observed in the MgH_2, while the sparking and instantaneous reaction is similar to $LiBH_4$. The results of the Surface Contact Test are shown in Figure 4b, where it can be seen that the material is immediately reactive with the water soaked filter paper. The bubble evolution prior to ignition is consistent with MgH_2, while the actual reactive event was seen with both constituent materials. Finally, the Water Drop Test, Figure 4c, shows a material that is highly reactive with the addition of a few drops of water with respect to a relatively large amount of the hydride material. The mixture is instantly reactive, much like $LiBH_4$ while the reaction takes several minutes to completely burn out, which is similar to MgH_2.

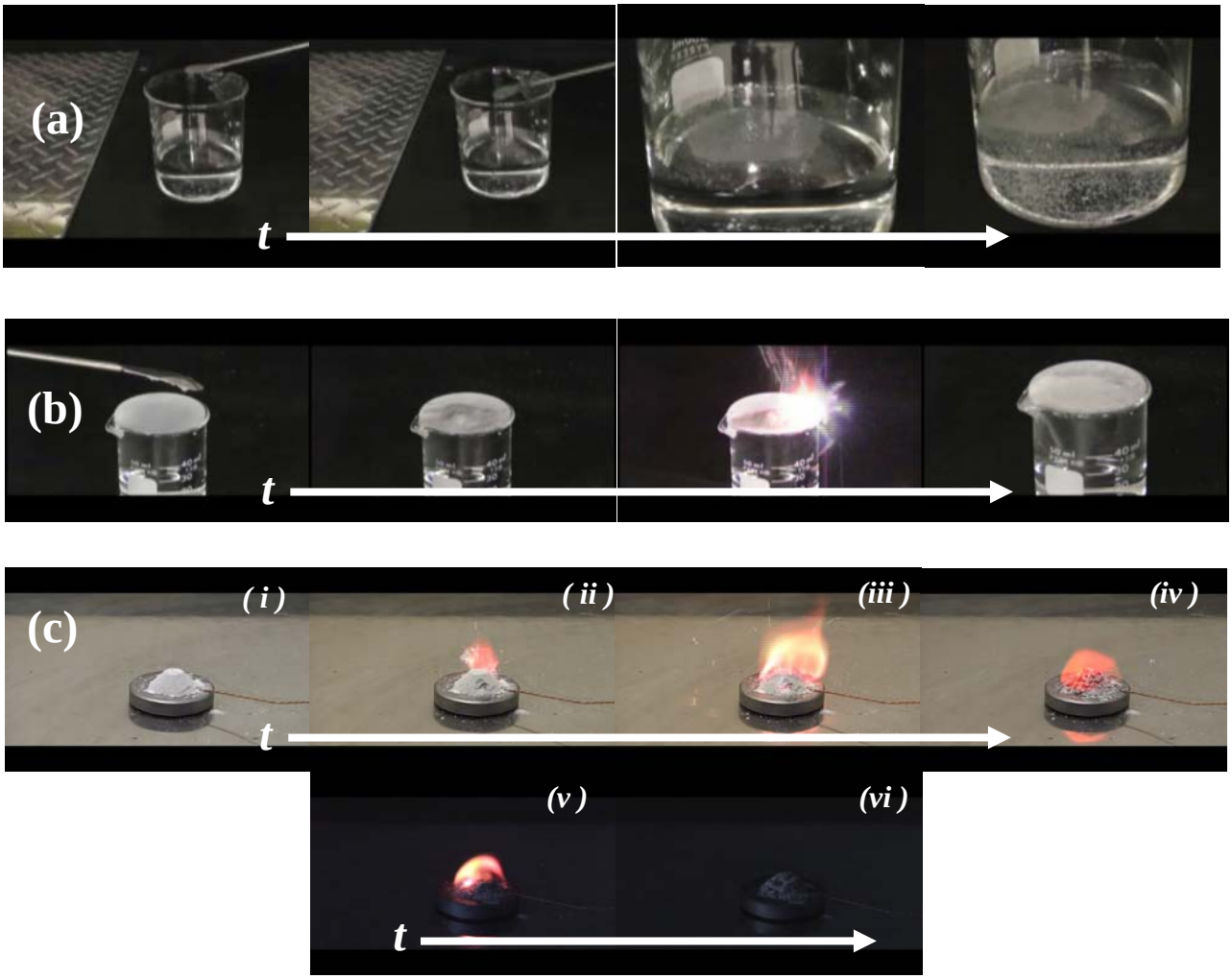

Figure 4 - Water reactivity results for (a) Water Immersion (b) Surface Contact, and (c) Water Drop Test for $2LiBH_4 \cdot MgH_2$. Time Increases from Left to Right.

In addition, the Water Drop test was slightly modified to record temperature data at a location underneath the pile. The maximum temperature reached was approximately 180 ^oC after 4 minutes at which time the temperature began to decrease. The temperature reached near-room temperature just after 10 minutes. Based on these results it is clear that the $2LiBH_4 \cdot MgH_2$ is reactive with water, as are the more well-known constituent materials $LiBH_4$ and MgH_2.

The difference in the observed water reactivity of $2LiBH_4 \cdot MgH_2$ compared to the parent materials is the result of different heat dissipation rates in the three scenarios and the rate of

hydrogen generation. In the Water Drop Test, hydrogen gas is rapidly evolved via the hydrolysis of the constituent $LiBH_4$ and MgH_2 materials; additionally, elemental Mg and Li may also be present in these samples after the ball milling process. These hydrolysis reactions are well known to be highly exothermic, and therefore the possibility of reaching the ignition temperature of the H_2 is possible. In the Water Drop Test, there is no appreciable heat sink to reduce the temperature of the sample and surrounding air. Comparing this to the Water Immersion Test, hydrogen gas is clearly evolved via hydrolysis, as in the Water Drop Test. However, with the presence of the relatively large amount of water in intimate contact with the material, the heat is more quickly wicked away thus preventing a reactive event. The Surface Contact Test is a hybrid between the two scenarios, where the mass transport of the water to the hydride for reaction is impeded by the presence of the filter paper, as is the transfer of the heat to the water which is restricted to only the bottom surface of the pile through the filter. It is obvious that this material is sufficiently reactive to build up enough heat energy and H_2 to give rise to an ignition event.

The $2LiBH_4{\cdot}MgH_2$ was also tested using the procedure for the U.N. Pyrophoricity classification, Figure 5. Approximately 1g of the material was dropped into a box with glass sides with the bottom made from industrial grade aluminum sheeting. The test nominally stipulates a 5 min waiting period. No reaction of the material in the air during the material drop, or within 15 minutes after the material was allowed to remain on the ground, was observed. Therefore, the material is deemed to be non-pyrophoric by the metrics used in this test.

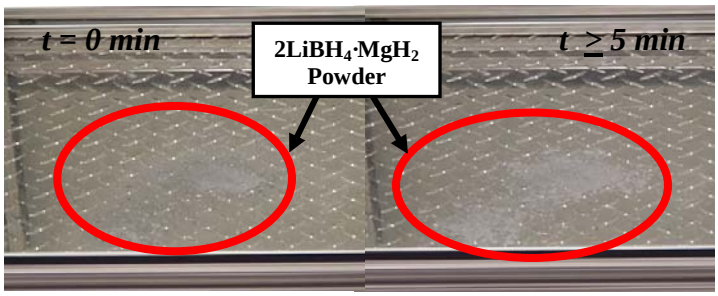

Figure 5 - Results from the Pyrophoricity Test for $2LiBH_4 \cdot MgH_2$.

The results of the Self-Heating Test for $2LiBH_4 \cdot MgH_2$ are shown below in Figure 6. Data were collected at 5 minute intervals during this experiment. A background control experiment was performed on a SiO_2 sample which was loaded into the sample container and placed into the oven. The test was started at room temperature (t = 0 min); however, after 5 minutes the highest reading is experienced at the face-center location (T = ~400°C), with the 2nd highest temperature at the corner (T = ~320°C), and the temperature at the center of the sample relatively low at T = ~240°C). It should be noted that the criterion for failure of the self-heating test is for the sample to heat above the ambient temperature by 60°C or more; thus the sample has already experienced dangerous self-heating at this point in the experiment. After the passage of another 5 minutes, the temperature of the center is now the highest measurement (T = ~410°C), followed by the temperature of the corner (T = ~340°C), followed by the temperature of the face-center (T = ~290°C). As time proceeds, the center increases until a maximum reading of ~450°C, after which the sample cools until it reaches a steady state of approximately 150°C, consistent with the background temperature from the SiO_2 sample. These results are interpreted as the procession of a reaction front, which starts at the face-center thermocouple, then proceeds towards the slightly more interior corner thermocouple, and finally to the central thermocouple. The relative insulation surrounding the central couple, provided by the reacted material, causes the couple to retain more heat and reach higher temperatures. These results are consistent with

temperature enhanced hydrolysis and oxidation of the hydride materials resulting from the contact with the ambient air in the oven at the elevated temperature of the test.

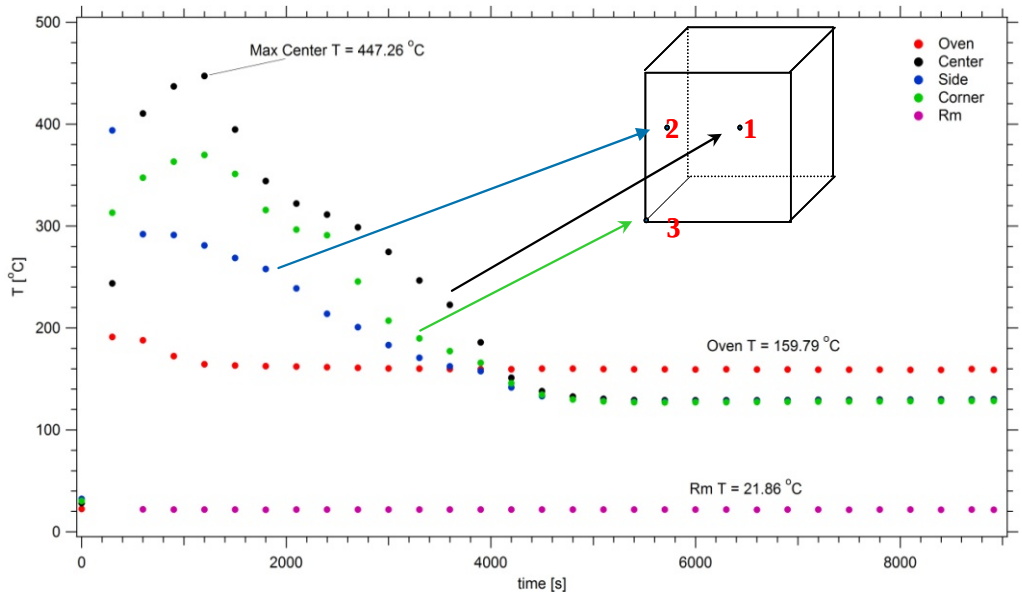

Figure 6 - Thermocouple readings for the Self-Heating Test performed on $2LiBH_4 \cdot MgH_2$. (Red = Oven Temperature, Black = Sample Center Temperature, Blue = Sample Side Temperature, Green = Sample Corner Temperature)

Figure 7 shows the results of the Burn Rate Test for the $2LiBH_4 \cdot MgH_2$ material. In Figure 7a, a photograph is shown which was taken ~ 5 s into the burn rate test, after which time the flame had propagated the entire length of the sample. It is obvious that the material is combustible by the metrics employed in this test. In Figure 7b, the results of the thermocouple measurements are shown as a function of time. In the upper right of the figure is an inset showing a blown-up depiction of the initiation period from 750s – 800s. The burn rate reported uses an average of the time optically measured using the video recording data, and the time measured using the thermocouple results. The calculated burn rate for this experiment was 52 mm/s. This value is very similar to the value previously measured for $NaAlH_4$ by Mosher *et al* of 51 mm/s. The lack of symmetry in the thermocouple measurements between the couples

which are reflectively displaced from the midpoint of the sample length axis is attributed to spatial non-uniformity of the sample during the test.

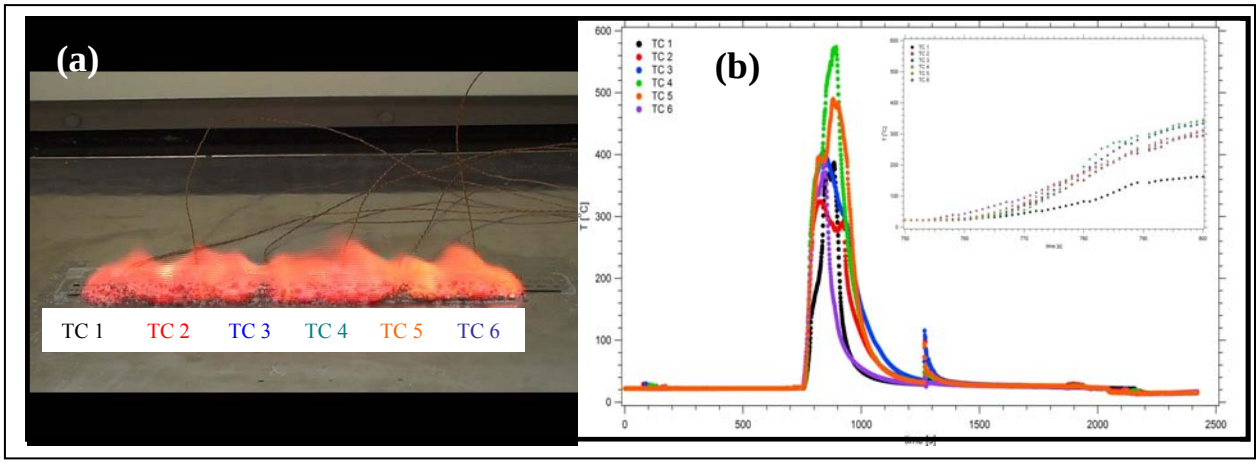

Figure 7 - Results of the Burn Rate Test for the $2LiBH_4 \cdot MgH_2$ material. a) Photograph of Burning Material after 5 seconds, b) Thermocouple Readings.

The findings of the current modified U.N. testing procedures for $2LiBH_4 \cdot MgH_2$ are summarized in Table 1, along with the results of the individual pure constituent materials.

Table 1: Results of the U.N. Standardized Tests for charged $2LiBH_4 \cdot MgH_2$

Material / UN Test	Pyrophoricity	Self-Heat	Burn Rate	Water Drop	Surface Contact	Water Immersion
MgH_2	Not Tested	Not Tested	Not Tested	2 H_2O drops required for near-instant ignition.	Material ignited	No ignition event recorded. Gas evolved at longer times. (5 min)
$LiBH_4$	Not Tested	Not Tested	Not Tested	2 H_2O drops required for near-instant ignition.	Material ignited	No ignition event recorded. Gas evolved at longer times. (5 min)
$2LiBH_4 \cdot MgH_2$	No ignition event. Hygroscopic material absorbed H_2O from air.	Self-heated ~300 ^oC within 5 min at as $T_{oven} = 150^oC$ is approached.	Flame propagated in 5 sec with burn rate of 52 mm/sec.	2 H_2O drops required for near-instant ignition.	Material ignited	No ignition event recorded. Gas evolved at longer times. (5 min)

3.2 Calorimetry

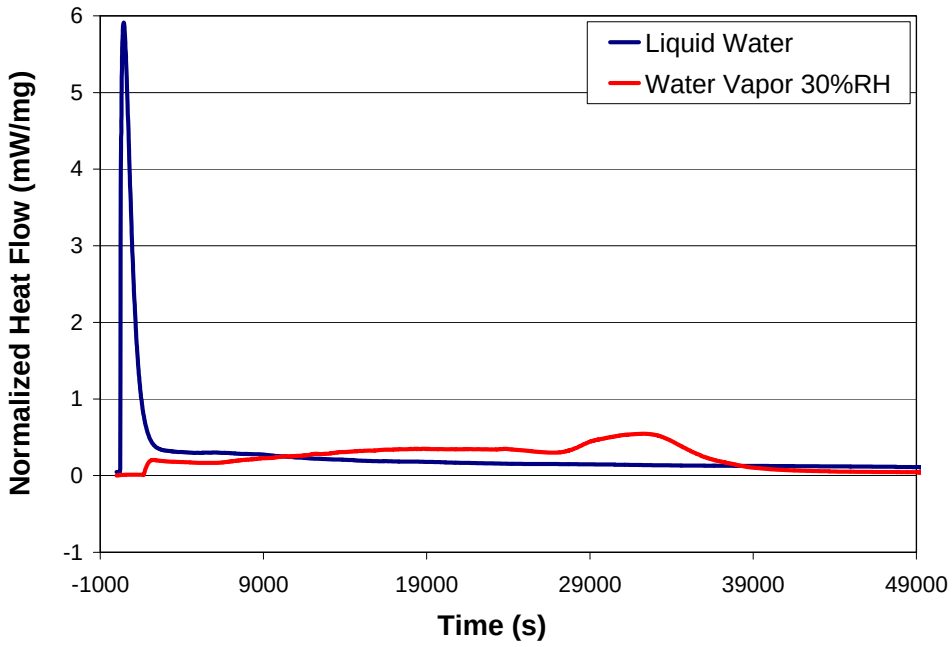

Figure 8 - Normalized heat flow (mW/mg) during hydrolysis/oxidation of $2LiBH_4 \cdot MgH_2$ with liquid water at 40°C and with 30% relative humidity air at 40°C (10 ml/min flow rate).

Figure 8 displays the normalized heat flow (mW/mg) for the $2LiBH_4 \cdot MgH_2$ reaction with liquid water in a mixing cell compared with water vapor in a gas flow cell. From Figure 1a it is seen that the amount of water addition in excess of stoichiometry is 32 times for liquid water and 4 times greater after a reaction time of 12 hours for the conditions of 40°C and 30% relative humidity. The qualitative difference observed in heat flow is believed to be due to the difference in gas/solid versus liquid/solid interfacial reactions. The total energy released through the water vapor reaction was greater (-268 kJ/mol) than the energy release upon liquid water hydrolysis (-223 kJ/mol). In addition the final crystalline reaction products were different in the two cases: the reaction with 30% relative humidity air resulted in $LiB(OH)_4$ and residual MgH_2, while the liquid water hydrolysis resulted in $LiB(OH)_4$, $H_6B_2O_6$ and $LiB(OH)_2(O_2)$. .

Table 2 summarizes the liquid mixing and gas flow reaction experiments performed both on the pure component $LiBH_4$ and MgH_2 as well as the destabilized mix ($2LiBH_4 \cdot MgH_2$) materials. Overall, in both the liquid mixing and gas flow reactions the trend is for a lower measured energy compared to the thermodynamically predicted reactions. A corollary to this is that the actual observed products do not match those predicted from thermodynamics and often have a significant degree of amorphous character.

An apparent anomaly in Table 2 for the reaction of liquid water with $LiBH_4$ is the actual measured ΔH (-320 kJ/mol) which is greater than the reaction for the theoretical lowest energy product predicted from the thermodynamic database. However the ΔH for the theoretical product does not take into consideration the heat of dissolution in aqueous solution of $LiBH_4 \rightarrow Li^+ + BH_4^-$ with an enthalpy of ~ 43 kJ/mol at 40^oC . In addition, the actual products were found to be amorphous lithium plus boron hydroxide product indicating a different reaction pathway occurred than thermodynamically predicted. The hydrolysis and oxidation of magnesium hydride was found to be extremely slow with starting material found in the final product and total measured heat of reaction less than 1% of those experimentally predicted. This is believed to be due to the relatively high stability of the $Mg(OH)_2$ surface layer (ΔH formation -334 kJ/mol).

Table 2: Experimental versus Theoretical Products and Reaction Energies

Material System	**Environmental Exposure**	**Theoretical Product** ΔH (kJ/mole) at 40°C	**Actual Product** ΔH (kJ/mole) at 40°C
$LiBH_4$	H_2O (liquid)	$LiBO_2$ -258	Amorphous Li + $B(OH)_3$ -320
	H_2O (gas) + **O_2 *air***	$LiOH + H_3BO_2$ -1386	$LiB(OH)_4 + H_6B_2O_6 + LiB(OH)_2(O_2)$ -352
	H_2O (gas) + ***Argon***	$LiBO_2$ - 344	$LiB(OH)_4$ -340
MgH_2	H_2O (liquid)	$Mg(OH)_2$ -278	$Mg(OH)_2 + Mg + MgH_2$ <-1
	H_2O (gas) + **O_2 *air***	$Mg(OH)_2$ - 848	$Mg + MgH_2$ <-1
Fully Charged $2LiBH_4{\cdot}MgH_2$	H_2O (liquid)	LiOH +1/2 $Mg(OH)_2$ $+H_3BO_2$ -445	Amorphous Li + $LiB(OH)_4$ + $Mg(OH)_2$ + Lithium borate hydrates -223
	H_2O (gas) + **O_2 *air***	LiOH +1/2 $Mg(OH)_2$ $+H_3BO_2$ - 1206	$LiB(OH)_4 + MgH_2$ -268
Fully Discharged $2LiH \cdot MgB_2$	H_2O (liquid)	LiOH + $Mg(OH)_2$ + H_3BO_2 -761	Amorphous Li + $Mg(OH)_2$, $Mg_5(BO_3)O(OH)_5{\cdot}2H_2O$ + $MgB_{12}O_{19}(H_2O)_5$ -170
	H_2O (gas) + **O_2 *air***	LiOH +MgO + B_2O_3 - 1289	$Mg(OH)_2 + LiB(OH)_4 + LiOH{\cdot}H_2O$ -205

When humid air is used as the reactive gas, there are two competing reactions; that between the material and oxygen and between the material and water vapor in addition to the possibility of hydrogen oxidation in the presence of air. Consideration of these effects independently using thermodynamic database revealed that the air oxidation was the predicted

dominant reaction. As a way to experimentally verify the effect of oxidation versus gas phase hydrolysis, argon as a carrier gas with 30% relative humidity was used in the $LiBH_4$ material system as a control experiment. With humid air as the gas reactant, the predicted energy release of -1386 kJ/mol comes from oxidation, while use of the humid argon reactive gas predicts an energy release of -344 kJ/mol from gas phase hydrolysis. XRD analysis showed the major product to be the same from the two reactions, $LiB(OH)_4$ .However the reaction that occurred in the presence of air had small amounts of $H_6B_2O_6$ as well as $LiB(OH)_4(O_2)$, but exhibited only a slight increase in the total amount of energy released. Insufficient data on the heats of formation are available to perform a thermodynamic analysis of these reactions.

The results of maximum heat flow during environmental exposure scenarios are presented in Figure 9 for both mixing with liquid water and in humid air and argon gas flow experiments. The data indicate that it is not the oxidative effects of oxygen which are of greatest risk for promoting energy release in the $2LiBH_4 \cdot MgH_2$ system, but it is the presence of gaseous oxygen itself which can combine with the hydrogen released from hydrolysis that is the real danger in environmental exposure scenarios.

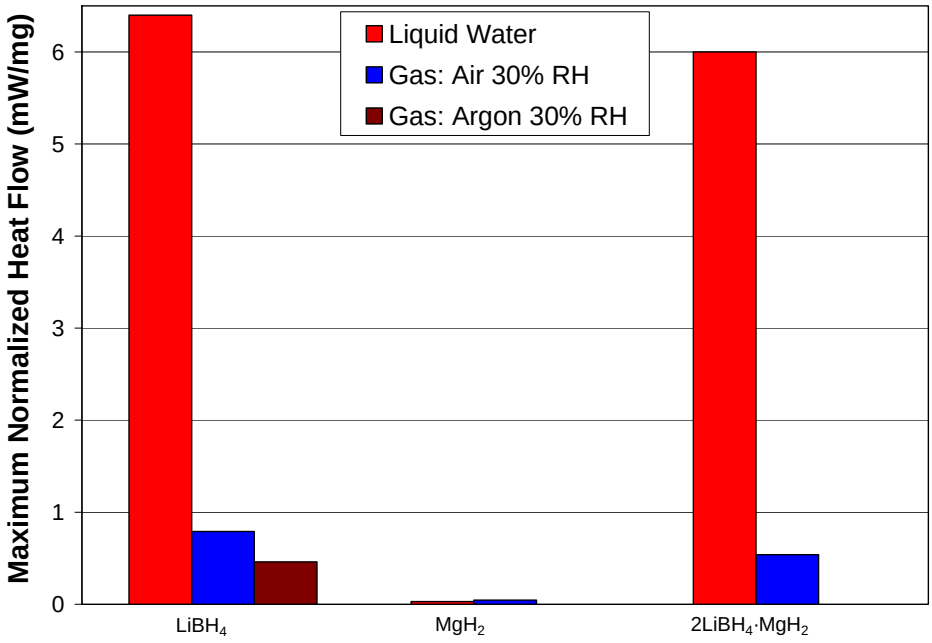

Figure 9 - Maximum rate of heat flow during hydrolysis at 40°C with liquid water, gas flow air with 30% relative humidity, and gas flow argon with 30% relative humidity.

Materials Charged State

Figure 10 presents the maximum heat flow for liquid phase hydrolysis at 40°C and 70°C as a function of the materials hydrogen charged state. The maximum heat flow increases as the material desorbs hydrogen and converts into more reactive LiH, Mg, and MgB_2 chemical compounds as predicted by the following chemical reactions:

$$LiBH_4 + 1/2MgH_2 + 4H_2O(l) = LiOH + \tfrac{1}{2}\, Mg(OH)_2 + H_3BO_2 + 4H_2(g) \quad \Delta H = -675 \text{ kJ/ formula unit} \qquad (2)$$

$$LiH + 1/2\, MgB_2 + 4\, H_2O(l) = LiOH + 1/2Mg(OH)_2 + H_3BO_2 + 2H_2(g) \quad \Delta H = -760 \text{ kJ/formula unit} \qquad (3)$$

Equations 2 and 3 represent the total amount of heat release expected for these reactions, while Figure 10 presents the rate of energy release, or maximum heat flux per mass of material (mW/mg). This data brings us to the important conclusion that the discharged material states are

more reactive to air and water exposure than the fully charged material states in the $2LiBH_4 \cdot MgH_2$ system. Risk assessments made in engineering design for storage tanks containing the $2LiBH_4 \cdot MgH_2$ material should take into account the discharged material states as a possible worst case estimate for environmental exposure scenarios.

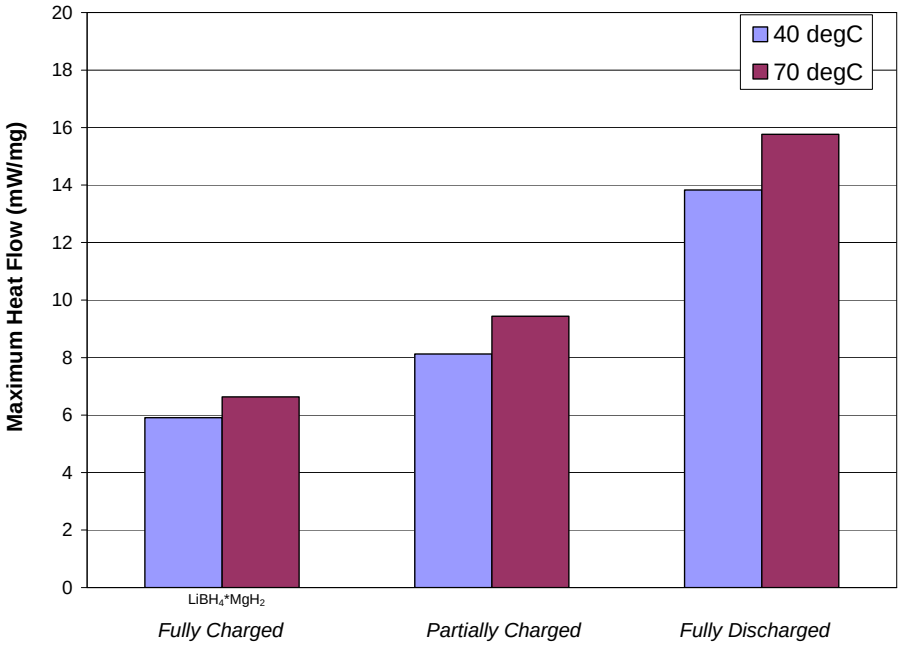

Figure 10 - Maximum heat flow (mW/mg) under liquid hydrolysis conditions as a function of temperature for fully charged, partially charged and fully discharged $2LiBH_4 \cdot MgH_2$

3.3 Heat/Mass Transfer in correlation b/w UN tests and Calorimetry: Predicting risk

The ultimate goal of the studies investigating the safety of hydrogen storage materials is to combine the physical property and reactivity data for the materials with modeling based on non-dimensional parameters and heat/mass transfer to predict hydrogen ignition, time to hydrogen ignition and probability that the hydrogen ignition will then pyrolyze and burn the remaining storage material. The first step in this direction is comparing the calorimetric data on liquid water mixing and humid air reactivity to the relevant UN tests. The time to ignition due to heat release, hydrogen release and oxygen present in the atmosphere may be estimated assuming the

thermal energy from the reaction is retained locally. For example, consider the time to ignition occurs when the energy release reaches 4.5 X 10^5 J/kg assuming this energy goes into raising the temperature of the material to the auto-ignition temperature of hydrogen (571^{o}C). The experimental value for the total energy release is determined by integrating the area under the heat flow curve as a function of time resulting in a curve of total energy release versus time. The time where this curve reaches 4.5 X 10^5 J/kg is the predicted time to ignition.

Liquid Water Contact

The experimental data for liquid water contact by calorimetry was based on an excess of water added at some initial time t = 0. The UN surface contact test most closely resembles this scenario where at t=0, the material is added to a wet filter paper saturated with water provides excess water for the hydrolysis reaction. The integrated calorimetric data is presented in Figure 11a where the estimated energy was reached after approximately 40 seconds. Figure 11b displays the hydrogen ignition event observed in the UN tests which occurred after approximately 10 seconds.

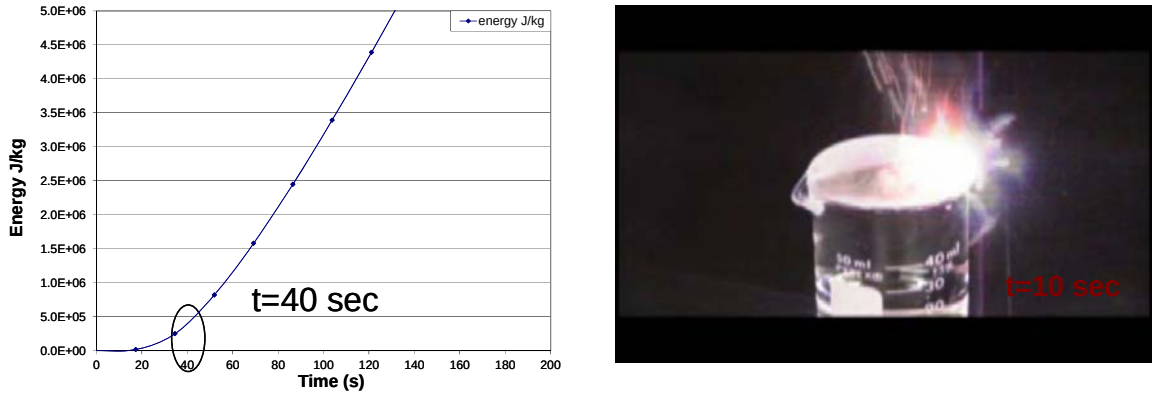

Figure 11 - a) Total energy release (J/g) determined by calorimetry as a function of time for liquid water hydrolysis at 40^{o}C of $2LiBH_4 \cdot MgH_2$ b) Surface Contact test with $2LiBH_4 \cdot MgH_2$ displaying a flame event after 10 seconds

Water Vapor Contact

The experimental data for water vapor contact by calorimetry was based on the amount of water vapor available for the hydrolysis reaction increasing as a function of time. The UN test which most closely resembles this was the pyrophoricity test where the material was dropped on the floor and exposed to ambient conditions in a fume hood with air circulation providing a flow rate of humid air across the material surface. The integrated calorimetric data is presented in Figure 12a where the estimated energy for ignition was not reached until over 1 hour of reaction. Figure 12b displays the image of the material after 15 minutes of air exposure stipulated in the UN test showing no indication of any flame event. Obviously at the long ignition time predicted, the assumption of adiabatic conditions is not valid. Due to the long exposure times and inevitable heat dissipation, the material cannot reach the auto-ignition temperature of H_2 (571^{o}C) and no flame event was observed

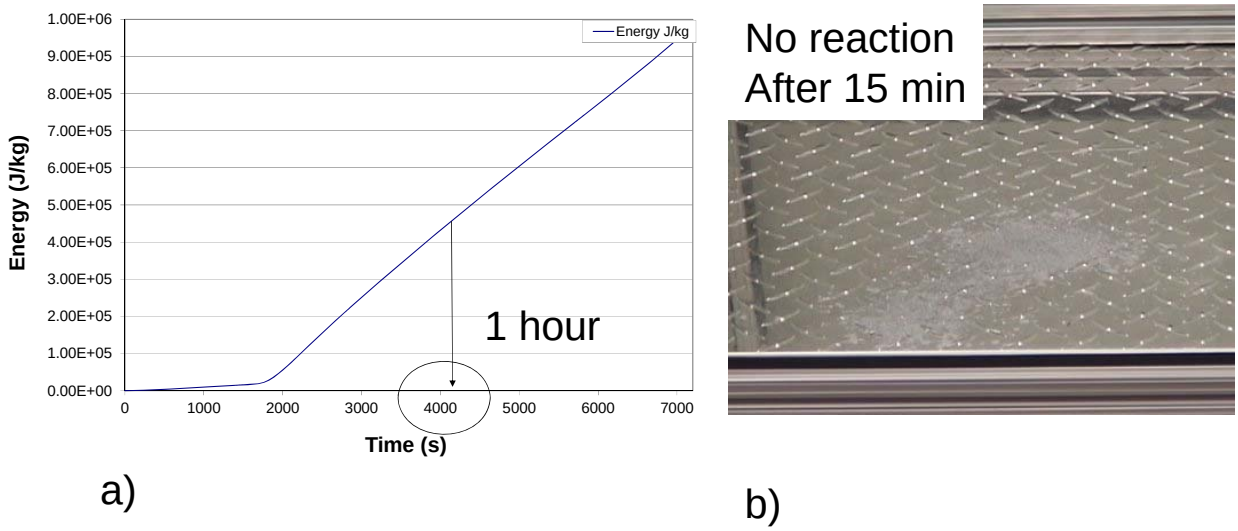

Figure 12 - a)Total energy release (J/g) determined by calorimetry as a function of time for water vapor hydrolysis at 40^{o}C and 30% relative humidity of $2LiBH_4 \cdot MgH_2$ b) Pyrophoricity test of $2LiBH_4 \cdot MgH_2$ displaying no flame event after 15 minutes.

4. Conclusions

The material $2LiBH_4 \cdot MgH_2$ has been evaluated using modified versions of United Nations test methodologies for shipping and packing classification. It was found that $2LiBH_4 \cdot MgH_2$ is reactive with both air and water under the conditions used in the current tests. The environmental reactivity of the destabilized $2LiBH_4 \cdot MgH_2$ system was most sensitive to water hydrolysis reactions with the destabilized mix following the behavior of the pure $LiBH_4$ component due to the relative lack of MgH_2 hydrolysis reactivity. A comparison of calorimetric data with relevant UN tests were used to develop the criteria for whether a given material will ignite based on the maximum heat flow and total energy released at times short enough to assume limited heat loss from the reaction system. The maximum normalized heat flow for the fully charged material was 6 mW/mg under liquid phase hydrolysis; and 14 mW/mg for the fully discharged material also occurring under liquid phase hydrolysis conditions. The experimentally observed products often contained significant amorphous content which are not reflected in the thermodynamic predictions. Finally, the dehydrogenated products were identified as having a higher potential heat release than the hydrogenated materials upon exposure to the environment, thus posing another risk factor in engineering hydrogen storage systems utilizing these materials.

Acknowledgements

The authors would like to thank David Missimer and Joseph Wheeler for their XRD and laboratory support, respectively. This work was funded under the U.S. Department of Energy Hydrogen Storage Program managed by Dr. Ned Stetson with whom many helpful and insightful discussions were held.

References

[1] Anton DL. Hydrogen desorption kinetics in transition metal modified NaAlH4. Journal of Alloys and Compounds 2003;356-357:400.

[2] Walters RT, Scogin JH. A reversible hydrogen storage mechanism for sodium alanate: the role of alanes and the catalytic effect of the dopant. Journal of Alloys and Compounds 2004;379:135.

[3] Bogdanovic B, Felderhoff M, Germann M, Härtel M, Pommerin A, Schüth F, Weidenthaler C, Zibrowius B. Investigation of hydrogen discharging and recharging processes of Ti-doped NaAlH4 by X-ray diffraction analysis (XRD) and solid-state NMR spectroscopy. Journal of Alloys and Compounds 2003;350:246.

[4] Züttel A, Wenger P, Rentsch S, Sudan P, Mauron P, Emmenegger C. LiBH4 a new hydrogen storage material. J Power Sources 2003;118:1.

[5] Züttel A, Rentsch S, Fischer P, Wenger P, Sudan P, Mauron P, Emmenegger C. Hydrogen storage properties of LiBH4. Journal of Alloys and Compounds 2003;356-357:515.

[6] Au M. Hydrogen Storage Reversibility of LiBH4 Based Materials. Presentation at the Fall 2005 MRS Meeting, Boston, MA, 2005.

[7] Pinkerton FE. Decomposition kinetics of lithium amide for hydrogen storage materials. Journal of Alloys and Compounds 2005;400:76.

[8] Song Y, Yang R. Decomposition mechanism of magnesium amide Mg(NH2)2. Int J Hydrogen Energy 2009;34:3778.

[9] Lu J, Choi YJ, Fang ZZ, Sohn HY. Effect of milling intensity on the formation of LiMgN from the dehydrogenation of LiNH2-MgH2 (1:1) mixture. J Power Sources;195:1992.

[10] Fisher M. Safety Aspects of Hydrogen Combustion in Hydrogen Energy-Systems. Int J Hydrogen Energy 1986;11:593.

[11] Mosher DA, Arsenault S, Tang X, Anton DL. Design, fabrication and testing of NaAlH4 based hydrogen storage systems. Journal of Alloys and Compounds 2007;446-447:707.

[12] Tanaka H, Tokoyoda K, Matsumoto M, Suzuki Y, Kiyobayashi T, Kuriyama N. Hazard assessment of complex hydrides as hydrogen storage materials. Int J Hydrogen Energy 2009;34:3210.

[13] Lohstroh W, Fichtner M, Breitung W. Complex hydrides as solid storage materials: First safety tests. Int J Hydrogen Energy 2009;34:5981.

[14] Vajo JJ, Skeith SL, Mertens F. Reversible Storage of Hydrogen in Destabilized LiBH4. J. Phys. Chem. B 2005;109:3719.

[15] Satyapal S, Petrovic J, Read C, Thomas G, Ordaz G. The U.S. Department of Energy's National Hydrogen Storage Project: Progress towards meeting hydrogen-powered vehicle requirements. Catalysis Today 2007;120:246.

[16] Fisher M. Safety Aspects in Hydrogen Energy Systems. Hydrogen Syst. Pap. Int. Symp. 1986;2:491.

[17] Hord J. How safe is hydrogen? Hydrogen Energy Distrib., Symp. Pap 1979:613.

[18] Green MA. Hydrogen Safety Issues Compared to Safety Issues with Methane and Propane. AIP Conference Proceedings, vol. 823, 2006. p.319.

[19] Ren R, Ortiz AL, Markmaitree T, Osborn W, Shaw LL. Stability of Lithium Hydride in Argon and Air. The Journal of Physical Chemistry B 2006;110:10567.

[20] Dedrick D, Behrens R, Bradshaw R. The Reactivity of Sodium Alanates with O2, H2O, and CO2. Sandia National Laboratory 2007;SAND2007-4960.

[21] United Nations Recommendations on the Transport of Dangerous Goods, Manual of Tests and Criteria, 3rd revised edition, 1999.
[22] http://www.setaram.com/C80-Cells.htm.
[23] James Jr CW, Tamburello DA, Brinkman KS, Gray JR, Hardy BJ, Anton DL. Environmental exposure of 2LiBH4+MgH2 using empirical and theoretical thermodynamics. Int J Hydrogen Energy 2011;36:2471.